

# The Scatterometer Climate Record Pathfinder

David G. Long  
Brigham Young University  
459 Clyde Building  
Provo, UT 84602  
long@ee.byu.edu

Mark Drinkwater  
ESA/ESTEC  
Postbus 299, 2200 AG  
Noordwijk, The Netherlands  
mark.drinkwater@esa.int

Benjamin Holt  
Jet Propulsion Laboratory  
MS 300-323  
Pasadena, CA 91109  
ben@pacific.jpl.nasa.gov

**Abstract**—While originally designed for ocean wind measurement, radar scatterometers have proven to be very effective in monitoring land cover and ice conditions and in climate studies. The NASA Scatterometer Climate Record Pathfinder (SCP) project has generated a unique climate data record from the series of historic and ongoing scatterometer missions. Image data are archived from the SeaWinds on QuikSCAT instrument, the scatterometer mode of the ERS-1/-2 AMI, the NASA Scatterometer (NSCAT), and the Seasat Scatterometer (SASS). In this paper we describe several SCP data sets and illustrate their application to studies of climate change over Greenland.

## INTRODUCTION

Radar scatterometers have been flown in space since the late 1970's with continuous data for the last decade. Originally designed to measure near-surface winds over the ocean, scatterometer data are also extremely useful in a broad range of ice and land applications, including studies of seasonal and inter-annual variability and possible relationships to climate change. Scatterometer data are currently being operationally used for iceberg tracking and sea ice extent mapping as well as for wind observation and numerical weather prediction. The frequent, global measurements of scatterometers make the instrument particularly well suited for global monitoring. Further, the long-time series of scatterometer measurements dating back to the Seasat scatterometer (SASS) in 1978 provide a valuable baseline for studies of climate change. For this reason the NASA Scatterometer Climate Record Pathfinder (SCP) project has produced an extensive set of scatterometer imagery and data products [5]. In this paper we describe some of these products and illustrate their application in a climate change study of the Greenland ice sheet.

## SCATTEROMETERS

A total of five different instruments have been flown, with two additional instruments to be launched soon. NASA has flown three scatterometers: the current SeaWinds scatterometer onboard the QuikSCAT satellite (QSCAT, 13.4 GHz) launched in 1999; the NASA scatterometer (NSCAT, 14.0 GHz) on the Japanese Space Agency's ADEOS-1 which operated 1996-1997; and the Seasat-A scatterometer system (SASS, 14.6 GHz) which flew for 3 months in 1978. The European Space Agency's (ESA) 5.3-GHz scatterometer (ESCAT) has been carried onboard both the ERS-1 and ERS-2 satellites since 1991, though useable

data ended in January 2001. A second SeaWinds instrument is planned for launch in late 2002 aboard ADEOS-II and ESA plans to launch ASCAT in the mid 2000's. ESCAT provides the longest continuous scatterometer record. Comparing ESCAT to NSCAT and QSCAT, which are at different frequencies, provides improved discrimination of scattering properties. The SASS provides a historical data set that can be compared with the remaining scatterometers to study decadal changes. The wide swath of scatterometers provides near-daily global coverage, particularly in the polar regions, at intrinsic resolutions generally between 25-50 km, over incidence angles ranging from 20-55 depending on the sensor.

A radar scatterometer transmits microwave pulses and receives the backscattered energy which depends on the roughness and dielectric properties of the target area. Scatterometers are very accurately calibrated, typically to better than a few tenths of a decibel (dB). For non-ocean areas, roughness properties and geometry that affect backscatter include surface roughness, moisture content, leaf size and density, branch orientation, and preferential alignment of surface scatterers. Dielectric properties are affected by physical characteristics of the effective scattering medium or layering such as snow grain size, brine concentration in sea ice, and canopy leaf density—as well as by the phase state of water (meltwater on sea ice and land ice, re-frozen percolated melt water in glacial ice, and whether trees are frozen or actively respiring). Due to the calibration accuracy and stability of scatterometers, seasonal and inter-annual differences that result in changes in the radar return as low as 1-2 dB may be confidently examined.

## AVAILABLE SCP PRODUCTS

As an aid in the application of scatterometer data to climate studies the SCP project is providing imagery from all these scatterometers in a unique, enhanced resolution format with additional value-added data products available. The SCP provides two basic forms of gridded image products: 1) backscatter images at the intrinsic sensor resolution and 2) enhanced resolution images which combines multiple overlapping passes over intervals of a few days. The latter are created using Scatterometer Image Reconstruction (SIR) algorithm [4]. The image pixel resolutions are 8.9 km/pixel for ESCAT, 4.45 km/pixel for SASS, NSCAT, and QSCAT with additional 2.225 km/pixel images for QSCAT. The enhanced products are well suited for many ice and land studies where the surface backscatter returns are comparatively stable over a 1-2 day period.

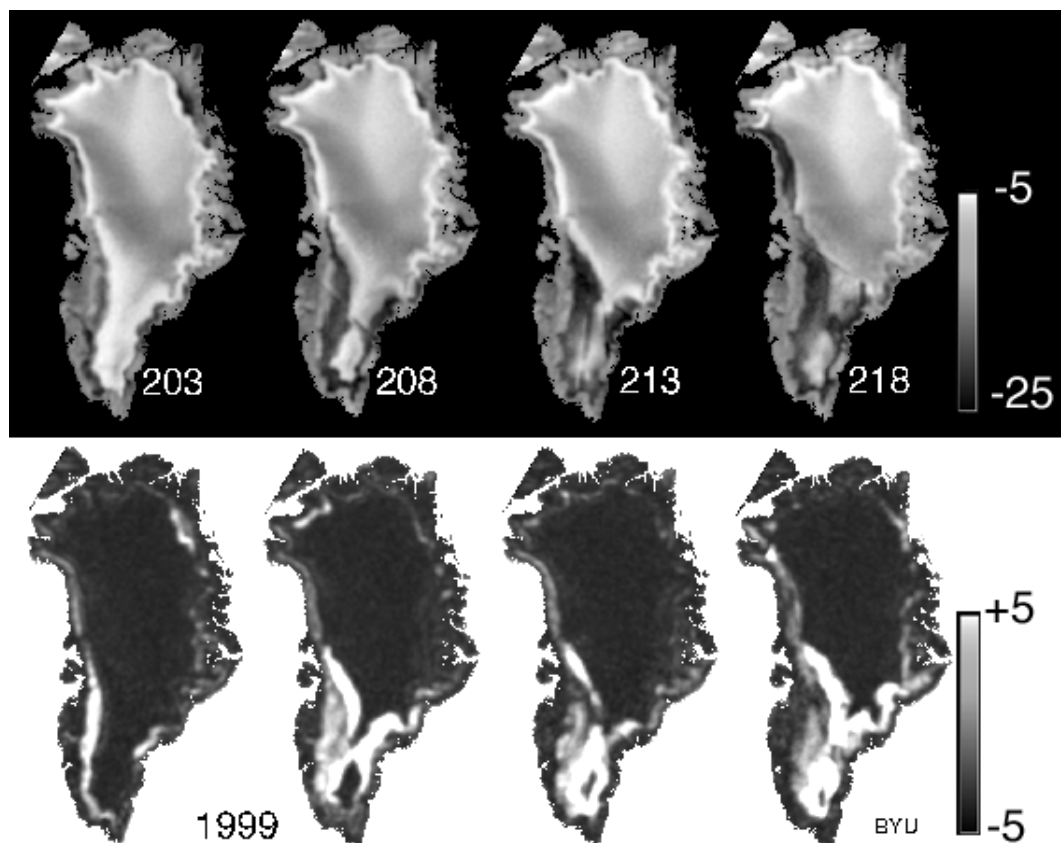


Fig. 1: Daily v-pol QuikSCAT “egg”  $\sigma^o$  (in dB) images of Greenland. (top) Evening passes. (bottom) Difference in  $\sigma^o$  (in dB) between morning and evening passes.

Scatterometer images, documentation, software, and other information are currently available through the SCP data site via the web at URL <http://www.scp.byu.edu/>. Processing is done at Brigham Young University’s (BYU) Microwave Earth Remote Sensing (MERS) Laboratory. QSCAT browse imagery and raw data are available from the Jet Propulsion Laboratory’s (JPL) Physical Oceanography Distributed Active Archive Center (PODAAC) (<http://podaac.jpl.nasa.gov/>). The PODAAC will eventually mirror all SCP products as well as provide options for obtaining the data on different media.

### POLAR ICE

Scatterometer data has been remarkably effective in polar climate studies (see [2, 6] for a recent summary). The daily global coverage of scatterometer data in the polar regions and its ability to discriminate sea ice, ice sheets, and icebergs, despite the variable solar illumination and frequent cloud cover, make scatterometer data an excellent instrument for large-scale systematic observations of polar ice. Both science and operational applications for the scatterometer data have been developed.

QSCAT images are currently being operationally used at the National Ice Center for tracking large icebergs in the Southern Ocean. Tabular icebergs made of glacial ice generally exhibit a high contrast with surrounding ocean and/or sea ice and are

thus easily identified. Due to QSCAT’s broad coverage, large tabular icebergs can be tracked on a daily basis.

Scatterometer backscatter over sea ice is sensitive to roughness and physical properties and has a distinct response compared to open ocean. NOAA NESDIS is operationally using polarization differences to separate ice and ocean from QSCAT image products for near real-time products. The onset of seasonal snow melt and freeze-up dramatically modifies the ice backscatter over sea ice. These events are significant transitions in the radiative budget of ice-covered regions and increasingly early melt onset and later fall freeze-up may be related to a possible climate trend. Additional studies of sea ice include the derivation of ice velocity fields and ice-type classification. Ice velocity fields are important for estimating heat flux between the ocean and atmosphere, and for sea ice mass balance. Motion fields have been derived using scatterometer data with various algorithms. Several recent ice type studies have shown improved accuracy when scatterometer data are combined with passive sensor data.

### GREENLAND STUDIES

The sensitivity of scatterometer backscatter to the density and size of snow grains in the various ice facies, especially in the percolation zone and during summer melt, makes the data invaluable in studies of the Greenland and Antarctic ice sheets. A

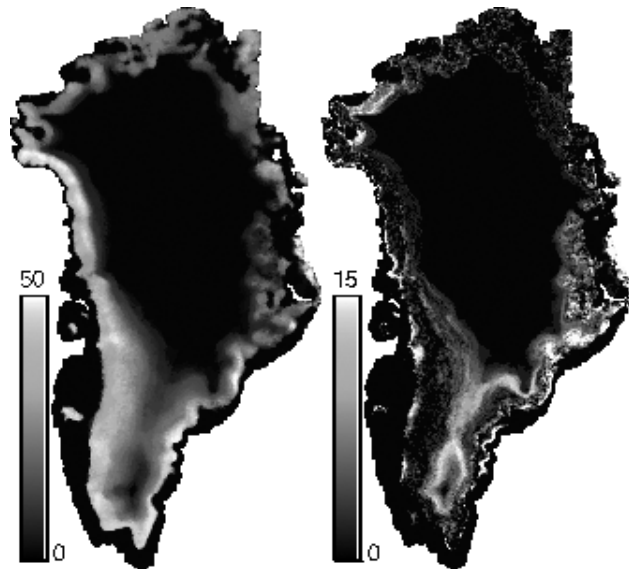


Fig. 2: QuikSCAT-derived days of melt after JD200 in 1999. (left) Descending passes. (right) Difference between ascending and descending passes.

time series of scatterometer images provide a means of examining long-term variability over the ice sheets, including the extent of the seasonal snow melt zone over Greenland and Antarctica [6]. By combining scatterometer data from multiple sensors, the long-term and inter-annual variability of accumulation rates and the extent of seasonal snow melt zones have been estimated over Greenland [3].

Determining the length of the melt is key in estimating ablation relating to the mass balance of the Greenland ice sheet. Seawinds makes it possible to measure the melt extent of the entire ice sheet daily and even observe diurnal variations.

Figure 1 shows an example of summer melt observed by Seawinds. The top images show  $\sigma^0$  during the time that the melt was extending to its farthest reach that year. Each image is created using only measurements from descending passes (evening local time). The area where melt is occurring is readily visible, especially in the southern region of the ice sheet. Where melt is occurring, the backscatter is reduced dramatically producing the dark areas in the image. This effect occurs even if only small amounts of liquid water are present.

The image time series at the bottom of Fig. 1 are difference images from morning to evening. The diurnal variation is very pronounced, indicated by the bright areas which appear mostly on the southern portion of the ice sheet. In comparing the descending images to the difference images, it is observed that at the higher elevations, the ice sheet is frozen in the morning, but beginning to melt by evening. At the lower elevations, the melt persists throughout the previous night. The yearly melt extent and duration is calculated from the Seawinds images using a simple variable threshold technique [1]. Figure 2 shows the total melt from JD200 onward observed by Seawinds during

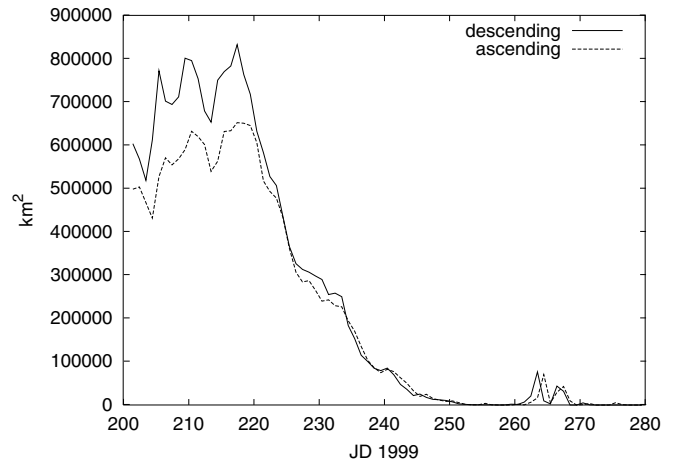


Fig. 3: QuikSCAT-derived melt area versus Julian Day, 1999.

1999. The image on the left shows the melt duration calculated from descending h-pol images only. The image on the right is the difference between the melt duration calculated from descending images and ascending images. Thus, it shows the number of partial melt days, or the days the ice sheet was frozen in the morning, but melting by evening.

The total extent of the melt is shown in Fig. 3. As expected, the melt extent in the morning is generally smaller than in the evening. By JD 252, the melt period is finished with the exception of a small melt event between JD 260 and 270.

#### Acknowledgments

The Scatterometer Climate Record Pathfinder task is supported by NASA's Office of Earth Science Enterprise through Research Announcement 99-OES-04. ESCAT data were provided by CERSAT-IFREMER as part of ESA Project AO2.USA.119.

#### REFERENCES

- [1] I.S. Ashcraft and D.G. Long, SeaWinds Views Greenland, *Proc. IGARSS'2000*, pp. 1131-1133, Hilton Hawaiian Village, Honolulu, HI, 24-28 July 2000.
- [2] M.R. Drinkwater and C. C. Lin, Introduction to the special section on emerging scatterometer applications, *IEEE Trans. Geosci. Remote Sens.*, vol. 38, pp. 1763-1764, 2000.
- [3] M.R. Drinkwater, D.G. Long, and A.W. Bingham, Greenland snow accumulation estimates from scatterometer data, *J. Geophys. Res.*, vol. 106, pp. 33935-33950, 2001.
- [4] D.S. Early and D.G. Long, Image reconstruction and enhanced resolution imaging from irregular samples, *IEEE Trans. Geosci. Remote Sens.*, vol. 39, pp. 291-302, 2001.
- [5] D.G. Long, M.R. Drinkwater, B. Holt, S. Saatchi, and C. Bertioia, Global Ice and Land Climate Studies Using Scatterometer Image Data, *EOS, Trans. AGU*, vol. 82, pg. 503, 23 Oct. 2001.
- [6] D.G. Long and M.R. Drinkwater, Cryosphere applications of NSCAT data, *IEEE Trans. Geosci. Remote Sens.*, vol. 37, pp. 1671-1684, 1999.